

# Regional soil erosion risk assessment in Hai Basin

LI Xiaosong, WU Bingfang, WANG Hao, ZHANG Jin

*Institute of Remote Sensing Applications, Chinese Academy of Science, Beijing 100101, China*

**Abstract:** Based on the experience of factors selection and integration for soil erosion monitoring, which were used in USLE, we evaluated the soil erosion risk in the Hai Basin and analyzed its spatial distribution under the support of RS and GIS. The results show that soil erosion risk in the mountainous area is remarkably higher than that in the plains area. In different mountain regions, soil erosion risk was highest in the Taihang Mountain area, lowest in the Beisanhe Mountain area, and the upstream of the Yongdinghe River has a level between them. Low soil erosion risk is located mainly in the plains area of gradients less than 5°, medium and higher risk are situated mostly in the areas with a gradient between 8° and 15° or 15° and 25°, which accounts for 65% of the total. The percentage of high soil erosion risk area increased as the slope gradient increased. Paddy fields have a lower soil erosion risk, and scrublands and grasslands are the primary land-use types with medium and high soil erosion risks, accounting for approximately 59.67%. In the future, water and soil conservation experts should focus on high soil erosion risk areas in order to create effective preventive measures.

**Key words:** USLE, remote sensing, GIS, soil erosion risk

**CLC number:** TP79

**Document code:** A

**Citation format:** Li X S, Wu B F, Wang H and Zhang J. 2011. Regional soil erosion risk assessment in Hai Basin. *Journal of Remote Sensing*, 15(2): 372–387

## 1 INTRODUCTION

For a long time, with the joint influence of natural factors (*e.g.*, concentrated rainfall, steep topography, loosen soil, and low vegetation coverage) and social factors (*e.g.*, large population intensity, reclamation on steep slopes, indiscriminate felling, and overgrazing), soil erosion already has become one of the most serious environmental issues in the Hai Basin (Ma, 2002).

Understanding the current soil erosion status is necessary for determining the scientific steps to take that will prevent soil erosion and to evaluate water and soil conservation effects objectively. Many efforts have been made to map soil erosion at different scales and in different regions around the world, which can be divided into qualitative and quantitative methods. Erosion models, which describe soil erosion process and result in quantitative outcomes, were adopted world-wide. The drawbacks of erosion models are the fixed data requirements, the fact that models are developed for a certain region, scale, and specific processes, and the difficulty in validating results (Vrieling, *et al.*, 2008). However, for local water and soil conservation agencies, getting an indication of the spatial distribution of erosion is enough in some cases, such as in conservation prioritization. Soil erosion risk, which usually indicates the relative probability that erosion will occur in one location as compared to other locations in the region mapped, can depict soil erosion intensity differences. Therefore, carrying out soil erosion

risk assessment has important practical significance at the regional scale, as well as identifying the spatial differences of soil erosion risk, which can be used to allocate scarce conservation resources and to develop policies and regulations.

Supported by the remote sensing (RS) and GIS techniques, soil erosion controlling factors were quantitatively determined at the regional scale, and then soil risk assessment in the Hai Basin was conducted in order to understand the current soil erosion risk spatial distribution and to provide the decision-making support for local administrative agencies.

## 2 STUDY AREA

The Hai Basin is located west of the Bohai Sea and east of the Taihang Mountain area, with the Yellow River as its southern border and the Mongolian Plateau as the northern border (Fig. 1). The study area is the Hai Basin, whose total area is 232000 km<sup>2</sup>, excluding the Luanhe River and the Tuhai River. The topography of the region consists mainly of a mountainous area in the north and west, which accounts for 58.37% of the total area, and plains in the south and east. The climate generally is characterized as a temperate zone with East Asia monsoon weather and annual average rainfall of 539 mm. Most of the rainfall occurs during the flood season from June to September.

In the area around Beijing and Tianjin, the Hai Basin has the

**Received:** 2010-06-02; **Accepted:** 2010-08-02

**Foundation:** The Knowledge Innovation Program of the Chinese Academy of Sciences (No. KZCX1-YW-08-03).

**First author biography:** LI Xiaosong(1981— ), male, Associate Professor, E-mail:lixs@irsa.ac.cn

**Corresponding author biography:** WU Bingfang, E-mail:wubf@irsa.ac.cn

specific feature of a large population and insufficient farmland areas, which has lead to reclamation on steep slopes to different extents. At the same time, most of the mountainous area has a thin layer of topsoil and low vegetation coverage. Combined adverse natural and social factors lead to severe soil erosion in the Hai Basin. Based on the national second soil erosion survey, a 105500 km<sup>2</sup> area had experienced soil erosion in the Hai Basin by the end of the 20th century, which accounts for 33.2% of the total basin. Water erosion is the dominant soil erosion type, with an area of 987200 km<sup>2</sup>, accounting for 94% of the total soil erosion area (Ma, 2002). Therefore, the status of soil erosion in the Hai Basin is serious, which is a grave threat to sustainable development of Hai Basin.

### 3 DATA AND METHOD

#### 3.1 Base data

The soil erosion controlling factors, which include rainfall, topography, vegetation, and soil characteristics, were collected in order to carry out soil erosion risk assessment at the region scale in the Hai Basin. The following datasets were collected:

(1) Rainfall data was downloaded from the China Meteorological Data Sharing Service System. This information includes monthly average rainfall data from 580 rain gauge stations in and around the Hai Basin from 2000 to 2008.

(2) Soil data was from the national second soil survey. This information includes soil types, soil mechanical composition, and soil organic matter content grid data, with a grid size of 2 km.

(3) Topography data was from SRTM DEM data, with a resolution of 90 m. This information was used to compute slope gradient and slope length.

(4) As NDVI is a good indicator of vegetation, the MODIS NDVI dataset from 2001 to 2008 was used in the study. The spatial

resolution was 1 km, and the time interval was 16 days.

(5) Land use data, a key factor to soil erosion, was from the Data Center for Resources and Environmental Sciences, CAS. It was produced based on 250 m MODIS data from 2005, with a scale of 1:250000.

#### 3.2 Methods for soil erosion risk assessment

Soil erosion risk is the qualitative expression of soil erosion rate, which places emphasis on intensity differences for different regions. In this sense, the methods of soil erosion risk assessment at the regional scale at least should be adaptable, objective and feasible at the region scale. The universal soil loss equation (USLE) is one of the least data-demanding erosion models. The USLE and its modified version (RUSLE: Renard, *et al.*, 1997) already have been used worldwide in different spatial scales and different environments (Jurgens & Fander, 1993; Van der Knijff, *et al.*, 2000; Ma, *et al.*, 2003). Although the equation has many shortcomings and limitations, such as being extrapolated from an empirical model, scale differences, and finiteness of considered soil erosion processes, it is used widely because of its relative simplicity and robustness. It also represents a standardized approach.

The factors used in the equation are objective, acquirable at the regional scale, and indicative of soil erosion controlling factors. Therefore, this equation is especially suitable for soil erosion risk assessment at the regional scale. We have evaluated the average soil erosion risk in the Hai Basin since 2000, based on the factor selection experience of USLE. The basic form of the USLE is as follows.

$$A=R \times K \times LS \times C \times P \tag{1}$$

where *A* stands for estimated soil loss (t/(hm<sup>2</sup>·a)), *R* is the rainfall and erodibility index (MJ·mm/(hm<sup>2</sup>·h·a)), *K* is the soil erodibility factor (t·hm<sup>2</sup>·h/(MJ·mm·hm<sup>2</sup>)), *LS* is the topographic factor (unitless),

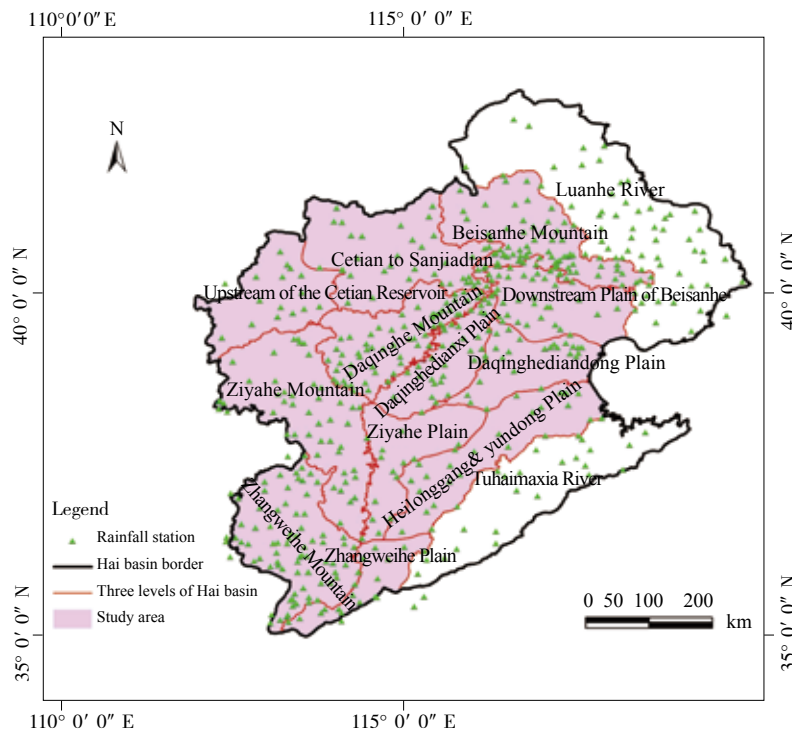


Fig. 1 Location of study area and distribution of rainfall station

$C$  is the cropping factor (unitless), and  $P$  is the conservation practice factor (unitless). The key to applying USLE is to determine the value of every factor in the equation. How to generate the map of every factor using RS and GIS technology is the key step in this study.

### 3.3 USLE factors calculation

#### 3.3.1 Rainfall erosivity index ( $R$ )

Rainfall erosivity index ( $R$ ) is a kinetic index which assesses soil detachment and transportation caused by rainfall, and reflects the potential capacity of rainfall to cause erosion. Based on the availability of rainfall data, we calculated average rainfall erosivity from 2000 to 2008 using monthly average rainfall and an empirical equation as follows (Wang, *et al.*, 1995):

$$R = \sum_{i=1}^{12} \left\{ 1.735 \times 10 \left( 1.5 \times \lg \frac{P_i^2}{P} - 0.818 \right) \right\} \quad (2)$$

where  $P_i$  stands for monthly average rainfall,  $P$  stands for yearly average rainfall, and the unit of rainfall erosivity is the metric unit, MJ·mm/(hm<sup>2</sup>·ha).

Average monthly and yearly rainfall data of different periods were calculated using the monthly rainfall data for the Hai Basin. Then an average precipitation spatial distribution map of every month and every year was interpolated using the Kriging interpolation method. Finally, the average rainfall erosivity index ( $R$ ) was calculated based on Eq. 2 (Fig. 3(a)).

#### 3.3.2 Soil erodibility factor

The factor  $K$  is defined as the amount of eroded soil per unit area cost by unit rainfall erosivity, which reflects different soils' erosion rates when other factors that influence erosion are constant. The physical properties of soil, such as texture, size, and stability of the structure, clay type, permeability, organic matter content, and soil thickness, affect soil erosion rates. Many researchers have studied soil erodibility factor estimation, but a method proposed by Wischmeier, a calculation method in EPIC, and an equation established by Shirazi, *et al.* are the most representative (Zhang, *et al.*, 2007).

The selection of different calculation methods depends on the availability of soil property data. Based on the national second soil investigation data,  $K$  was calculated using the same method as William, *et al.* in the EPIC model (USDA, 1990):

$$K = \left\{ 0.2 + 0.3 \exp[0.0256 SAN(1 - SIL/100)] \right\} \times \left( \frac{SIL}{CLA + SIL} \right)^{0.3} \times \left( 1.0 - \frac{0.25C}{C + \exp(3.72 - 2.95C)} \right) \times \left( 1.0 - \frac{0.7SN_1}{SN_1 + \exp(-5.51 + 22.9SN_1)} \right) \quad (3)$$

where  $C$  stands for soil organic carbon content,  $SAN$  is sand content,  $SIL$  is silt content,  $CLA$  is clay content, and  $SN_1 = 1 - SAN/100$ . In addition,  $K$  (calculated using the method mentioned above) was modified based on the research by Zhang so as to be consistent with the practical situation of China. The modified equation is as follows.

$$K = -0.01383 + 0.51575K_{epic} \quad (4)$$

The distribution of factor  $K$  in the Hai Basin is as seen in Fig. 3(b).

#### 3.3.3 The slope length and steepness factor ( $LS$ )

The impact of topography on soil erosion is concentrated on slope length and steepness. Therefore, slope length and steepness typically are used to estimate the influence of topography on soil erosion, which are both accelerators of rainfall erosivity. The  $LS$  factor was calculated with improved slope length factor and slope steepness factor based on the procedure proposed by Wischmeier and Smith. The equation is as follows:

$$L = (\lambda / 22.13)^m \quad (5)$$

where  $L$  stands for the slope length factor,  $\lambda$  is horizon slope length, and  $m$  is the exponent related to slope length. Slope length is determined through the calculation of upslope drainage area. The two equations are expressed as follows:

$$\begin{cases} m = \beta / (1 + \beta) \\ \beta = (\sin \theta / 0.0896) / [3.0(\sin \theta)^{0.8} + 0.56] \end{cases} \quad (6)$$

$$\lambda = D / \cos \theta = \text{Flow Accumulation} \times \text{Cell Size} \quad (7)$$

where  $\theta$  stands for slope steepness,  $D$  is slope length in pixel scale, and  $\text{Cell Size}$  is the size of pixel.

The equation used to calculate slope steepness factors depends on the steepness of the slope; namely, for a gentle slope, we used the equation proposed by McCool; for a steep slope, we used the equation proposed by Liu Baoyuan. The equations are combined below (McCool, *et al.*, 1989; Liu Baoyuan, *et al.*, 1994):

$$S = \begin{cases} 10.8 \sin \alpha + 0.03 & \alpha < 5^\circ \\ 16.8 \sin \alpha - 0.5 & 5^\circ \leq \alpha < 10^\circ \\ 21.9 \sin \alpha - 0.96 & \alpha \geq 10^\circ \end{cases} \quad (8)$$

where  $S$  stands for slope steepness factor, and  $\alpha$  is slope steepness. The spatial distribution of the  $LS$  factor in the Hai Basin is shown in Fig. 3(c).

#### 3.3.4 Cropping and management factor ( $C$ )

The cropping and management factor ( $C$ ) for the USLE is defined as the ratio of soil loss from land cropped under specific conditions to the corresponding loss from clean-tilled, continuous fallow, which acts as an inhibitor to erosivity. The cropping and management factor ( $C$ ) is an important factor in the USLE model and is used to control soil erosion intensity. Due to its variability and large amplitude of variations, it becomes a factor that is difficult to calculate quantitatively. The calculation of the  $C$  factor at the regional scale usually relies on a lookup table and is defined in terms of land use. This method, however, can not accommodate the difference in land use; neither can it reflect the differences such as vegetation condition or tillage measures brought by phenophase. In this study,  $C$  was determined using the form of NDVI proposed by Jones. The average  $C$  factor from 2000 to 2008 in the Hai Basin was calculated based on coarse resolution NDVI data.

$$C_i = \exp \left( -\alpha \times \frac{(\text{NDVI})_i}{\beta - (\text{NDVI})_i} \right) \quad (9)$$

where  $\alpha$  and  $\beta$  are the parameters deciding the shape of the curve. Many applications suggest that the ideal results were acquired when  $\alpha=2$  and  $\beta=1$ . Even though some questions exist in the  $C$  calculation with the vegetation index, this method is one of the simplest and most practical to obtain  $C$  at the regional scale. The average NDVI of the flood season (from June to Oc-

tober) in the corresponding time range was calculated first, and then the  $C$  factor distribution map was produced using Eq. 9, as shown in Fig. 3(d).

### 3.3.5 Conservation practices factor

The conservation practices factor is defined as the ratio between the soil losses expected for a certain soil conservation practice and that of up-and-down slope plowing (Liu, et al., 2001). At present, the value of the  $P$  factor in runoff plots typically is determined by experimental observation. However, determining the related parameters is difficult through the experiments at the regional scale. Land use/

land cover can reflect the differences of conservation to some extent, so the value of  $P$  usually is appointed according to land use types. In this study, the value of  $P$  was determined by referring to the research results of Cai, et al. in combination with local land use and farming activities (Table 1). Land use data was provided by the Data Center for Resources and Environmental Sciences Chinese Academy of Sciences with a map scale of 1: 250000, which was drafted based on MODIS data. These data were taken as average conditions of conservation factor  $P$  from 2000 to 2008 in the Hai Basin (Fig. 3(e)).

**Table 1**  $P$  Value of different land use types

Land use type	Paddy field	Dry land	Woodland	Sparse woodland	Other forestry	Shrub land	Water areas	Urban settlement	Bare rock
$P$ value	0.01	0.4	1	1	0.7	1	0	0	0

## 3.4 Soil erosion risk assessment

When calculating different soil erosion control factors, some differences exist in the spatial scale due to the different data resources. Firstly, the layers mentioned before were transformed into the same grid size (1 km  $\times$  1 km) and projected into uniform coordinate system, and then all factors were multiplied to obtain the soil erosion map. Even though the quantitative result was acquired, we conducted the qualitative classification based on the histogram (Fig. 2) and other research results (Ouyang & Pan, 2006; Li, et al., 2010), when considering the scale differences and the application objective. Through the classification, the different soil erosion risk grades that describe relative probability were acquired. Subsequently, the soil erosion risk differences in different regions were analyzed using the statistical analysis. The erosion modulus threshold of the different grades and areas of different grades are shown in Table 2.

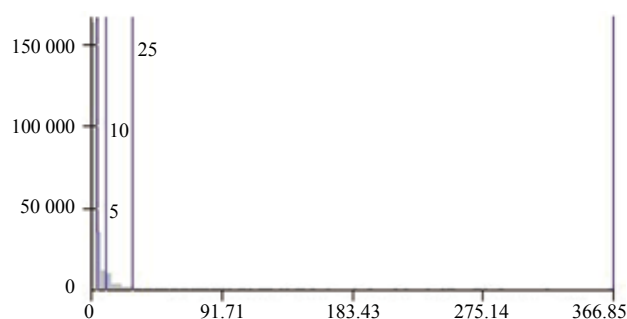


**Fig. 2** Soil erosion modulus histogram in Hai Basin

**Table 2** Soil erosion risk rate and statistics for the Hai Basin

Erosion modulus $/(t \cdot hm^{-2} \cdot a^{-1})$	Soil erosion risk rate	Area $/km^2$	Percentage $\%$
0—5	Very low	159079	69.13
5—10	Low	50025	21.74
10—25	Medium	19534	8.49
> 25	High	1480	0.64

## 4 RESULTS AND ANALYSIS

### 4.1 Spatial distribution of soil erosion risk

The soil erosion risk grade distribution in the Hai Basin is shown in Fig. 3f. Four grade classes from very low to high exist in the Hai Basin. To illustrate the soil erosion risk distribution in detail, the soil erosion risk grade map was analyzed by overlaying it with three levels of the Hai Basin. A distinct boundary between the mountainous areas and the plains areas could be seen. The soil erosion risk grade in the plains areas is very low. However, the soil erosion risk grade in the mountainous area increase clearly. By and large, the soil erosion risk in the Beisanhe mountainous area clearly is lower than in other mountainous areas, which indicates better prevention of soil erosion in the upstream of the Miyun Reservoir to some extent.

In order to analyze the differences in the soil erosion risk of mountainous areas, we firstly analyzed the soil erosion risk distribution of six three-level mountainous regions by statistics. The results are

shown in Table 3: high soil erosion risk area's distribution differs in different three-level mountainous regions, from high to low they are listed as the Zhangweihe mountainous area (426 km<sup>2</sup>), the Ziyahe mountainous area (347 km<sup>2</sup>), the Daqinghe mountainous area (230 km<sup>2</sup>), the section between the Cetian Reservoir and Sanjiadian (217 km<sup>2</sup>), upstream of the Cetian Reservoir in the Yongdinghe River (59 km<sup>2</sup>) and the Beisanhe mountainous area (28 km<sup>2</sup>). This indicates that high soil erosion risk exists in the Zhangweihe mountainous area, the Ziyahe mountainous area, the Daqinghe mountainous area, and the section between the Cetian Reservoir and Sanjiadian in Yongdinghe, more attention should be paid to these regions in the future. Besides, based on the percentage of medium and above soil erosion risk, the Daqinghe mountainous area has the highest soil erosion risk, with a percentage of 21.45%. Moreover, the area of low soil erosion risk exceeds very low risks by 2519 km<sup>2</sup>. The Ziyahe mountainous area and the Zhangweihe mountainous area take second place, with percentages of

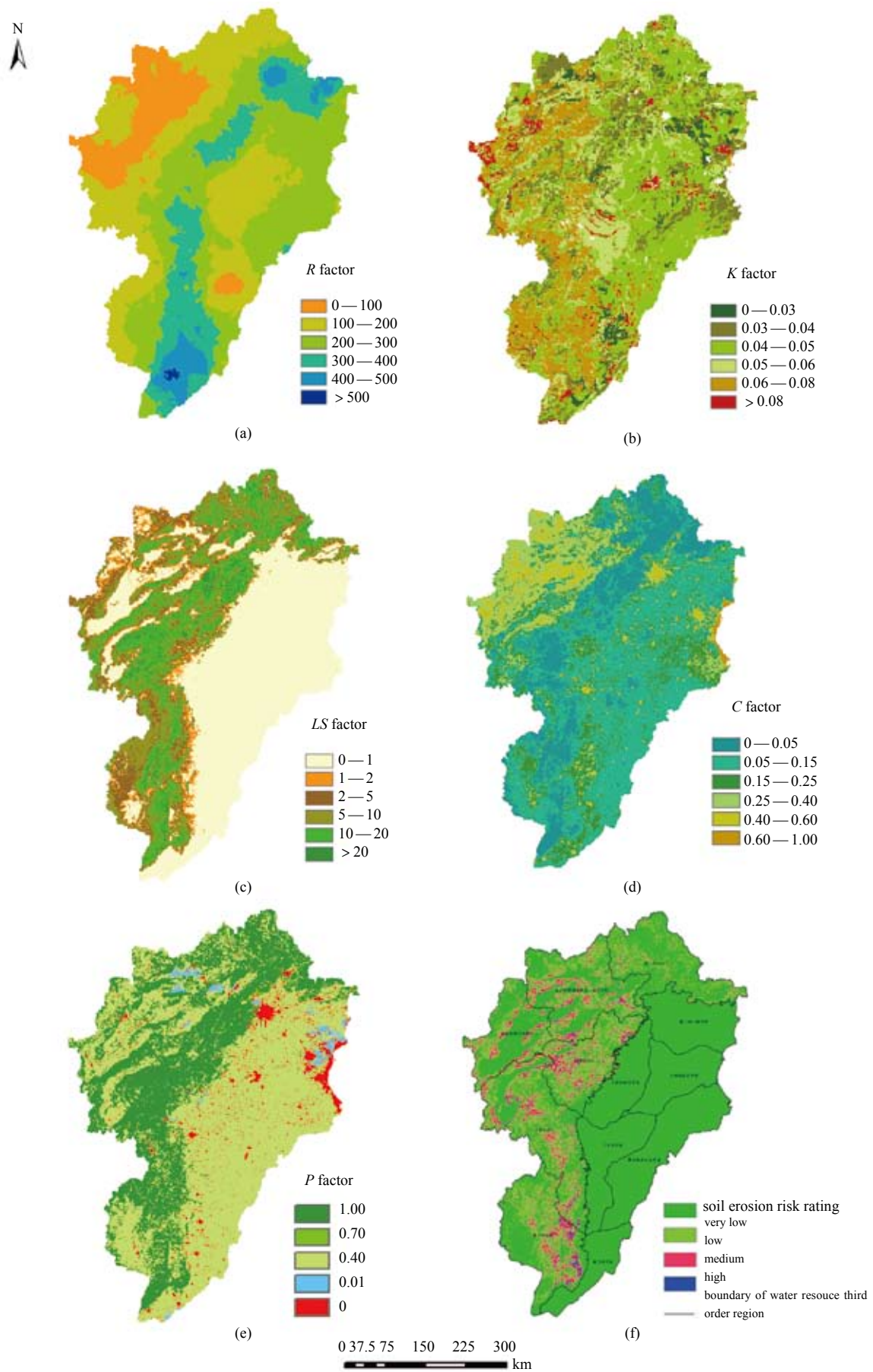


Fig. 3 Control factor and soil erosion risk maps

(a) Rainfall erosivity factor; (b) Soil erodibility factor; (c) Slope length and steepness factor; (d) Cropping and management factor; (e) Conservation practices factor; (f) soil erosion risk map



**Table 3 Area statistic of mountainous region soil erosion risks in Hai Basin**/km<sup>2</sup>

Water Resource Three Level Region (mountainous area)	Soil erosion risk rating				Percentage of medium and above
	Very low	Low	Medium	High	
Beisanhe	14453	6568	932	28	4.37%
Daqinghe	6015	8534	3744	230	21.45%
Upstream of the Cetian Reservoir in the Yongdinghe River	10449	4697	2102	59	12.49%
The section between the Cetian Reservoir and the Sanjiadian in the Yongdinghe River	14096	9042	3912	217	15.14%
Ziyahe River	13602	11750	4993	347	17.40%
Zhangweihe River	12725	9126	3750	426	16.05%

17.40% and 16.05%, respectively, followed by the section between the Cetian Reservoir and the Sanjiadian and upstream of the Cetian Reservoir in the Yongdinghe River, with percentages of 15.14% and 12.49%, respectively. The Beisanhe mountainous area, on the whole, has the lowest soil erosion risk, with a percentage of only 4.37%. In summary, soil erosion risk is the lowest in the Beisanhe mountainous area, highest in the Taihangshan mountainous area, and upstream of the Yongdinghe River falls between these risks.

## 4.2 Spatial difference character analysis

### 4.2.1 The relationship between the soil erosion risk and slope

Slope, which is an important factor in controlling soil erosion, directly affects the ability of runoff erosion. In order to analyze the conditions of soil erosion risk of different steepness in the moun-

tainous areas, we divided the slopes into six levels: 0° to 5°, 5° to 8°, 8° to 15°, 15° to 25°, 25° to 35°, and >35°. After this, an overlap analysis was conducted to determine the distribution soil erosion risk in different slope areas (Table 4). In terms of different soil erosion risk rating, the area of very low grade is located mainly in area slopes of less than 5°, and the medium- and high-risk areas are situated mostly in area slopes between 8° and 25°, which areas account for 65% of all the medium- and high-risk areas. Regarding different slopes, the percentage of high-risk grade increased from 0.09% to 2.1% as the slope increased. This indicates that the topography factor is an important factor leading to high soil erosion risk. Therefore, in the future, water and soil conservation should be focused on slopes between 8° and 25° in the Hai Basin. Meanwhile, high soil erosion risk areas of steeper regions should be given more attention.

**Table 4 Area statistics of soil erosion risk of different steepness**/km<sup>2</sup>

Slope	Soil Erosion Risk Rating			
	Very low	Low	Medium	High
<5°	125951	9330	2192	124
5°—8°	7418	8368	2772	135
8°—15°	11749	15959	6928	405
15°—25°	9840	12056	5743	458
25°—35°	3345	3586	1538	164
>35°	433	600	297	29

### 4.2.2 The relationship of soil erosion risk and land use

Analyzing the relationship between soil erosion risk and land use would help identify the land use types which are prone to soil erosion, which can provide support for later soil and water conservation. A tabulated analysis was conducted by overlapping the soil erosion risk and land use (Table 5). Based on these results, the soil erosion risk of a paddy field generally is very low, with 98.5%, and medium- and high-risk areas are located mostly in scrublands and grasslands, with 59.67%. Furthermore, low soil erosion risk areas are larger than very low soil erosion risk areas, which means scrublands and grasslands are prone to soil erosion. The next is woodlands, with 17.96%, followed by dry land and sparse woodlots, at 10.6% and 9.6%, respectively. Therefore,

scrublands and grasslands have the highest soil erosion risk, which should be custom controlled in the future.

## 5 CONCLUSION

Based on the experience of factor selection and integration of USLE, we evaluated the soil erosion risks in the Hai Basin using RS and GIS and drew the following conclusions:

(1) A distinct boundary clearly can be seen between the mountainous areas and plains areas. Soil erosion risk is very low in plains areas, but it increases significantly in mountainous areas. The soil erosion risk grades of very low, low, and medium are dominant,

**Table 5 Area statistics of soil erosion risks of different land uses**/km<sup>2</sup>

Land Use Type	Soil Erosion Risk Rate			
	Very low	Low	Medium	High
Paddy fields	526	7	1	0
Dry land	87687	6746	2109	110
Woodlands	11558	9550	3503	255
Sparse woodlots	4973	4684	1859	150
Scrublands and grasslands	25886	27488	11561	842
Others	28329	1518	491	46

while high soil erosion risks are distributed only on a local scale.

(2) From the perspective of percentage of medium and above soil erosion risk, the Daqinghe mountainous area has the highest soil erosion risk, with 21.45%. The Ziyahe mountainous area and the Zhangweihe mountainous areas' soil erosion risk were slightly lower, with 17.40% and 16.05%, respectively, then followed by the section between the Cetian Reservoir and Sanjiadian and upstream of the Cetian Reservoir in the Yongdinghe River, with 15.14% and 12.49%, respectively. The Beisanhe mountainous area, on the whole, has the lowest soil erosion risk, with only 4.37%. Generally, soil erosion risk is the lowest in the Beisanhe mountainous area, highest in the Taihangshan mountainous area, and the upstream of the Yongdinghe River is between these risks.

(3) The areas of very low grade are located mainly in flat areas where slopes are less than 5°, medium and high-risk areas are situated mostly in the areas where slopes are between 8° and 25°, which accounts for 65% of all the medium and high-risk areas. The percentage of high-risk grade increases as the slope increases.

(4) The soil erosion risk of paddy fields is very low, with 98.5%, while high-risk areas are located mostly in scrublands and grasslands, which represent 59.67% of both the medium and high soil erosion risk areas. The next is woodland, with 17.96%, followed by dry land and sparse woodlots, with 10.6% and 9.6%, respectively. Therefore, scrublands and grasslands have the highest soil erosion risk, which should have customized controls in the future.

The Beisanhe mountainous area, the upstream of the Yongdinghe and the Taihangshan mountainous area all belong to the national key water and soil conservation project, but with different starting time. Among of which, the upstream of the Yongdinghe River project started first in 1982, followed by the upstream of the Miyun Reservoir project in 1989 and the Taihangshan mountainous area project in 1996 (Meng, 2004). Due to the effects of national investments and local economy, water and soil conservation can not be completed overnight but is a gradual process. Some differences are found in the time and efforts of the measures in different regions, which affect the soil erosion prevention projects and, in turn, are reflected by the soil erosion risk grade. As stated in section 4.1, the Taihangshan mountainous area has the highest soil erosion risk as a whole, which is caused directly by the large mountainous area, backward economies, and the shortage of water and soil conservation. The Beisanhe mountainous area, located in the upstream of the Miyun Reservoir, was managed later than the upstream of the Yongdinghe River. The Miyun Reservoir, however, is the only surface drinking water source for Beijing. Therefore, both the state and the city of Beijing have a big investment. That may explain why the Beisanhe mountainous area has a lower soil erosion risk than the upstream of the Yongdinghe River as a whole.

In the future, soil and water conservation investment will increase in the Hai Basin. However, the soil and water conservation methods must be scientific. With the limited resources and investments, the answers to the following questions will serve as the basis for scientific water and soil conservation: which kind of region is more prone to soil erosion; what kind of land use type has the highest soil erosion risk; and what kind of topography is most vulnerable to serious soil erosion? The distribution map of soil erosion risk we calculated in this study will be helpful in answering these questions and can provide support for decision-making by officials in admin-

istrative agencies of the Hai Basin.

## REFERENCES

- Cai C F, Ding S W, Shi Z H, Huang L and Zhang G Y. 2000. Study of Applying USLE and Geographical Information System IDRISI to Predict Soil Erosion in Small Basin. *Journal of soil and water conservation*, **14**(2):19–24
- De Jong, S M, Brouwer, L C and Riezebos, H. 1998. Erosion hazard assessment in the Peyne catchment, France. Working paper DeMon-2 Project. The Netherlands: Utrecht University: 8–18
- Jorgens C and Fander M. 1993. Soil erosion assessment and simulation by means of SGEOS and ancillary digital data. *International Journal of Remote Sensing*, **14** (15): 2847–2855
- Li X S, Ji C C, Wu B F, Zeng Y and Yan N N. 2010. Dynamics of water and soil loss based on remote sensing and GIS: A case study in Chicheng County of Hebei Province. *Chinese Journal of Ecology*, **28**(9): 1723–1729
- Liu B Y, Nearing M A and Risse L M. 1994. Slope gradient effects on soil loss for steep slopes. *Transactions of the ASAE*, **37**(6): 1835–1840
- Liu B Y, Xie Y and Zhang K L. 2001. *Soil Erosion Prediction Model*. Beijing: China Science and Technology Press: 163–200
- Ma J W, Xue Y, Ma C F, and Wang Z G. 2003. A data fusion approach for soil erosion monitoring in the Upper Yangtze River Basin of China based on Universal Soil Loss Equation (USLE) model. *International Journal of Remote Sensing*, **24** (23): 4777–4789
- Ma Z Z. 2002. Water and soil conservation ecological construction measures layout in view of the present situation of water and soil loss in the Haihe River Basin. *Haihe water resources*, (5):5–9
- McCool, D K, Brown L C, Foster G R, Mutchler C K and Meyer L D. 1989. Revised slope length factor for the Universal Soil Loss Equation. *Transactions of the ASAE*, **32**(5):1571–1576
- Meng X Z and Li Z X. 2005. Review and prospect of water and soil conservation monitoring in the Haihe Basin. *Haihe water resources*, (5):18–20
- Ouyang X Z and Pan J H. 2006. Quantitative Study of Soil Erosion on the Longdong Loess Plateau Using GIS and RS—A Case Study of the Qingcheng Project Area. *Bulletin of soil and water conservation*, **26**(5):75–81
- Renard K G., Foster G R, Weessies G A, McCool D K and Yoder D C. 1997. *Predicting Soil Erosion by Water: A guide to conservation planning with the Revised Universal Soil Loss Equation (RUSLE)*. U.S. Department of Agriculture, Agriculture Handbook: 703
- United States Department of Agriculture. 1990. EPIC-Erosion / productivity Impact Calculator 1. Model Documentation. Technical Bulletin Number 1768. Washington DC
- Van der Knijff J M, Jones R J A and Montanarella L. 2000. *Soil Erosion Risk Assessment in Europe*, EUR 19044 EN. Hannover: European Soil Bureau: 34
- Vrieling A, De Jong S M, Sterk G and Rodrigues S C. 2008. Timing of erosion and satellite data: A multi-resolution approach to soil erosion risk mapping. *International Journal of Applied Earth Observation and Geoinformation*, **10**(3): 267–281
- Wang W Z. 1995. Study on rainfall erosivity in China. *Journal of soil and water conservation*, **9**(4):5–18
- Wischmeier W H and Smith D D. 1978. *Predicting rainfall erosion losses—a guide for conservation planning*. U.S. Department of Agriculture, Agriculture Handbook: 537
- Zhang K L, Peng W Y and Yang H L. 2007. Soil erodibility and its estimation for agricultural soil in China. *Acta Pedologica Sinica*, **44**(1):7–13

# 区域尺度海河流域水土流失风险评估

李晓松, 吴炳方, 王浩, 张瑾

中国科学院 遥感应用研究所, 北京 100101

**摘要:** 借鉴USLE的因子选择及综合方法, 在遥感和GIS的支撑下对海河流域的水土流失风险进行评估, 并对其空间分布特征进行分析。结果表明: 海河流域山区水土流失风险显著高于平原地区, 北三河山区水土流失风险最低, 太行山区最高, 永定河上游介于两者之间; 水土流失风险“很低”等级主要分布在小于5°的平坦地区, “中”、“高”水土流失风险面积主要集中在8°—15°与15°—25°两个坡度带内, 约占总面积的65%, 且“高”水土流失风险面积所占比例随坡度的增加而增加; 水田的水土流失风险很低, “中”、“高”水土流失风险主要存在于灌草地类型上, 约占总“中”、“高”水土流失风险面积的59.67%。未来的治理应依据水土流失风险的高低有针对性地开展, 以达到事半功倍的效果。

**关键词:** USLE, 遥感, GIS, 水土流失风险

**中图分类号:** TP79      **文献标志码:** A

**引用格式:** 李晓松, 吴炳方, 王浩, 张瑾. 2011. 区域尺度海河流域水土流失风险评估. 遥感学报, 15(2): 372-387

Li X S, Wu B F, Wang H and Zhang J. 2011. Regional soil erosion risk assessment in Hai Basin. *Journal of Remote Sensing*, 15(2): 372-387

## 1 引言

长期以来, 受海河流域暴雨集中、地面坡度大、土质疏松和植被覆盖率低等自然原因以及人口密度大、陡坡开荒、滥砍乱伐、超载放牧和社会原因的综合影响, 水土流失已成为海河流域最为突出的生态环境问题之一(马志尊, 2002)。

为了科学、有效地防治水土流失, 客观评价水土流失治理效益, 必须查清水土流失的现状。当前, 国内外已围绕水土流失监测进行了大量工作, 大致可以分为定性与定量两大类。其中考虑水土流失过程的土壤侵蚀模型研究较多, 该方法通过经验模型或物理模型得到水土流失的定量结果, 但其最主要缺陷就是对数据输入要求较高, 只适合于特定区域、特定尺度和特定过程, 而且结果通常很难验证(Vrieling等, 2008)。然而, 对于区域管理机构而言, 掌握区域水土流失强度的空间差异即可满足需求。水土流失风险指区域中某处相比于其他位置水土流失可能发生的

相对概率, 其结果为从最低到最高的水土流失风险等级, 较好地反映了区域内水土流失强度的空间差异。因此, 开展区域尺度上水土流失风险评价研究, 对了解区域水土流失空间差异, 进而为稀缺水土保持措施的合理配置及水土保持政策的制定提供技术支持, 具有重要的现实意义。

在遥感和GIS技术的支撑下, 通过定量获取区域尺度水土流失控制因子的空间分布, 开展区域尺度上的海河流域水土流失风险评估, 以准确掌握当前海河流域水土流失风险的空间分布情况, 进而为流域管理机构防治水土流失提供决策支持。

## 2 研究区概况

海河流域东临渤海, 西倚太行, 南界黄河, 北接蒙古高原。本文研究区是除滦河和徒骇马颊河以外的海河水系, 总面积约23.2万km<sup>2</sup>。研究区地势西北高东南低, 西部和北部为山区, 山区面积约占总面积的58.37%。研

**收稿日期:** 2010-06-02; **修订日期:** 2010-08-02

**基金项目:** 中国科学院知识创新工程重大项目“重大工程生态环境效应遥感监测与评估”(编号: KZCX1-YW-08-03)。

**第一作者简介:** 李晓松(1981—), 男, 中国科学院遥感应用研究所助理研究员, 研究方向为土地退化遥感应用, 已发表相关论文10余篇。

E-mail: lixs@irsa.ac.cn。

**通信作者:** 吴炳方, E-mail: wubf@irsa.ac.cn。



究区位于温带东亚季风气候区,年平均降水量539 mm,降水主要集中在6月—9月的汛期。海河流域地处京畿要地,人口密度大、耕地少,因而存在着不同程度的陡坡开荒等问题,而且海河流域山区大部分土层浅薄,植被覆盖率不高,不利自然因素与社会因素的叠加使得水土流失在海河流域山区的表现尤为显著。

根据全国第二次遥感调查结果,20世纪90年代末,海河流域水土流失面积为10.55万 $\text{km}^2$ ,占流域总面积的33.2%。其中,水蚀面积9.872万 $\text{km}^2$ ,风蚀面积0.655万 $\text{km}^2$ ,工程侵蚀面积0.026万 $\text{km}^2$ ,水土流失形式以水蚀为主。由此可见,海河流域水土流失形势相当严峻,对海河流域可持续发展构成了严重威胁。

### 3 数据与方法

#### 3.1 基础数据

为开展海河流域水土流失风险评估,对降水、地形、植被和土壤等水土流失控制因子数据进行了收集,具体包括:

(1) 降水数据来自于中国气象科学数据共享服务网([2008-10-08]http://www.cdc.cma.gov.cn),共包括海河流域及其周边总计580个气象站自2000

年—2008年的月平均降水数据,气象站的分布如图1所示;

(2) 土壤数据来源于国家第二次土壤普查的相应数据,包括土壤类型及2 km格网上的土壤机械组成及有机质含量数据;

(3) 地形数据来自于SRTM DEM数据,分辨率约为90 m,用于坡度、坡长的计算;

(4) NDVI是植被的较好指示,本研究所用NDVI数据为MODIS NDVI数据集,时间分辨率为16 d,空间分辨率为1 km,时间范围为从2001年—2008年;

(5) 土地利用类型对水土流失影响较大,本研究所用土地利用数据来源于中国科学院资源环境科学数据中心,比例尺为1:250000,主要基于2005年250 m的MODIS数据制作。

#### 3.2 水土流失风险评估方法选择

水土流失风险是水土流失速率的定性化表达,其重点在于强调水土流失强度空间的强弱差异。因此,区域尺度水土流失风险评估的方法至少应具有可适性强、不受人为因素干扰和区域尺度评估指标可获取的特点。通用土壤流失方程(Universal soil loss equation, USLE)是所需变量最少的侵蚀模型

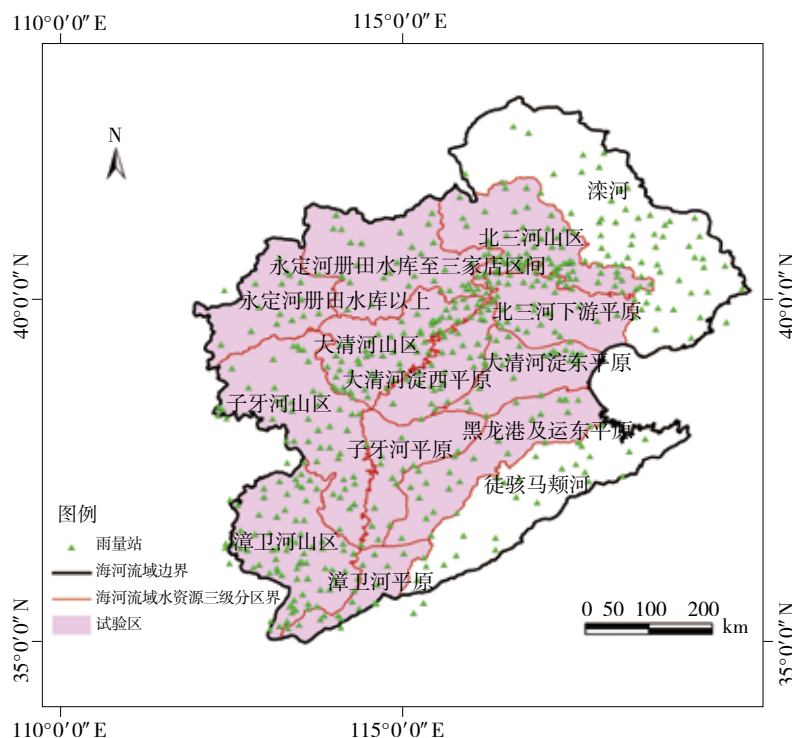


图1 研究区位置及雨量站分布图

之一，USLE及其改进版本（RUSLE：Renard 等，1997）已经被应用的世界范围内的不同空间尺度、不同环境和不同大小的区域（Jurgens和Fander，1993；Van 等，2000；Ma 等，2003）。尽管USLE存在着诸多缺点和不足，如经验模型的外推性、应用尺度的差异性和水土流失过程考虑的有限性等，但是USLE以其相对简单及稳定性得到了广泛的应用，可以说它代表了一种标准化的方法，而且其所用因子具有明确的指示性、客观性以及区域尺度可获取性的特点，因此该方法对区域尺度上的水土流失风险评估尤为适用。因此，本研究借鉴USLE的因子选择、计算与综合方法，对海河流域2000年以来的平均水土流失风险进行评估。USLE的基本形式如式（1）：

$$A=R \times K \times LS \times C \times P \quad (1)$$

式中， $A$ 为土壤侵蚀量（ $t \cdot hm^{-2} \cdot a^{-1}$ ）， $R$ 为降雨侵蚀力因子（ $MJ \cdot mm \cdot hm^{-2} \cdot h^{-1} \cdot a^{-1}$ ）， $K$ 为土壤可蚀性因子（ $t \cdot hm^2 \cdot h \cdot MJ^{-1} \cdot mm^{-1} \cdot hm^{-2}$ ）， $LS$ 为坡长、坡度因子， $C$ 为覆盖与管理因子， $P$ 为水土保持措施因子。应用USLE的关键是确定方程各因子指标值，利用遥感和GIS技术进行水土流失各因子图的生成是本研究的关键所在。

### 3.3 海河流域不同时期USLE因子计算

#### 3.3.1 降雨侵蚀力因子（ $R$ ）

降雨侵蚀力因子 $R$ 是一项评价降雨引起的土壤分离和搬运的动力指标，反映了降雨对土壤侵蚀的潜在能力。基于研究区雨量资料的可获得性，本研究直接利用多年各月平均降雨量推求 $R$ 值的经验公式计算了2000年—2008年的多年平均降雨侵蚀力（王万忠，1995）：

$$R = \sum_{i=1}^{12} \left\{ 1.735 \times 10 \left( 1.5 \times \lg \frac{P_i^2}{P} - 0.818 \right) \right\} \quad (2)$$

式中， $P_i$ 为各月平均降雨量（mm）； $P$ 为年平均降雨量（mm），降雨侵蚀力单位为公制单位（ $MJ \cdot mm \cdot hm^{-2} \cdot h^{-1} \cdot a^{-1}$ ）。

利用海河流域多年的月降水数据，计算不同时期的月平均降水量及年平均降水量，采用Kriging插值法进行空间内插得到不同时期各月平均降水量及年平均降水量的空间分布图，最后基于式（2）计算得到海河流域不同时期的多年平均降雨侵蚀力 $R$ （图2(a））。

#### 3.3.2 土壤可蚀性因子（ $K$ ）

$K$ 值定义为单位降雨侵蚀力在标准小区上造成的

土壤流失量，反映了在其他影响侵蚀的因子不变时，不同类型土壤所具有的不同的侵蚀速度。土壤的物理特性（如土壤质地，结构的大小及稳定性、黏粒类型、土壤的渗透性、有机质含量和土壤厚度等）影响着土壤的侵蚀速度。关于土壤可蚀性值估算的研究很多，具有代表性的成果为Wischmeier等人提出的方法、EPIC模型中的计算方法，以及Shirazi等人所建立的公式（张科利 等，2007）。

不同计算方法的选择主要决定于土壤属性数据的可获取性。本研究以国家第二次土壤普查数据为基础，采用William等人在EPIC模型中的方法计算 $K$ 值（USDA，1990）：

$$K = \left\{ 0.2 + 0.3 \exp \left[ 0.0256 SAN (1 - SIL/100) \right] \right\} \times \left( \frac{SIL}{CLA + SIL} \right)^{0.3} \times \left( 1.0 - \frac{0.25C}{C + \exp(3.72 - 2.95C)} \right) \times \left( 1.0 - \frac{0.7SN_1}{SN_1 + \exp(-5.51 + 22.9SN_1)} \right) \quad (3)$$

式中， $SAN$ 、 $SIL$ 、 $CLA$ 为沙粒、粉粒和黏粒含量（%）， $C$ 为土壤有机碳含量（%），除沙粒外其他成分含量 $SN_1 = 1 - SAN/100$ 。另外，基于张科利等人的研究成果，本研究对于利用EPIC计算得到的 $K$ 值进行修订，以使其更为符合中国的实际情况，修订公式如式（4）：

$$K = -0.01383 + 0.51575K_{epic} \quad (4)$$

海河流域的 $K$ 因子分布如图2(b)所示。

#### 3.3.3 坡度坡长因子（ $LS$ ）

地形地貌特征对土壤侵蚀的影响集中表现在坡长与坡度两方面，因此，一般用坡长（ $L$ ）与坡度（ $S$ ）因子估算地形因素对土壤侵蚀的影响，二者是降雨侵蚀动力的加速因子。其中，坡度因子是在其他条件相同的情况下，特定坡度的坡地土壤流失量与标准径流小区坡度的坡地土壤流失量之比；坡长因子则是在其他条件相同的情况下，特定坡长的坡地土壤流失量与标准径流小区坡长的坡地土壤流失量的比值。

$LS$ 的计算方法按照Wischmeier和Smith（1978）提出的程序，应用经过改进的坡长因子和坡度因子来进行海河流域每一个坡段 $LS$ 因子的计算，具体公式为：

$$L = (\lambda / 22.13)^m \quad (5)$$

式中,  $\lambda$ 为水平方向坡长;  $m$ 为与坡度相关的指数, 坡长通过累计汇水面积计算, 两者计算公式如式(6)和(7):

$$\begin{cases} m = \beta / (1 + \beta) \\ \beta = (\sin\theta / 0.0896) / [3.0(\sin\theta)^{0.8} + 0.56] \end{cases} \quad (6)$$

$$\lambda = D / \cos\theta = \text{流水累积量} \times \text{像元大小} \quad (7)$$

式中,  $\theta$ 为坡度(%);  $D$ 为像元尺度坡长; Cell Size为像元大小, 坡度因子的计算公式采用分段考虑, 即: 缓坡采用McCool坡度公式, 陡坡采用刘宝元的坡度公式合并表示为(McCool等, 1989; 刘宝元等, 1994):

$$S = \begin{cases} 10.8\sin\alpha + 0.03 & \alpha < 5^\circ \\ 16.8\sin\alpha - 0.5 & 5^\circ \leq \alpha < 10^\circ \\ 21.9\sin\alpha - 0.96 & \alpha \geq 10^\circ \end{cases} \quad (8)$$

式中,  $S$ 为坡度因子,  $\alpha$ 为坡度。最终计算的海河流域的 $LS$ 因子空间分布如图2(c)所示。

### 3.3.4 植被覆盖与管理因子( $C$ )

USLE中定义的植被覆盖与管理因子 $C$ 值是指, 在一定条件下, 有植被覆盖或实施田间管理的坡地土壤流失量与同等条件下实施精耕的连续休闲地土壤流失量的比值。它是侵蚀动力的抑制因子, 起着保持水土的作用。植被覆盖与管理因子 $C$ 是USLE模型中控制土壤流失强度的一个重要影响因子, 以其值的多变性和变化幅度之大成为USLE中定量计算难度较大的一个因子。区域尺度上 $C$ 因子的计算通常基于查找表的方法根据不同土地利用予以指定,

然而该方法无法反映土地利用内部之间的差别, 也不能反映区域尺度上物候期不同所带来植被状态和耕作措施等差异的影响。本研究参考De(De等, 1998)提出的以NDVI指数形式计算 $C$ 的方法, 基于区域尺度上分辨率较低的遥感植被指数NDVI资料计算海河流域2000年—2008年的平均 $C$ 因子:

$$C_i = \exp\left(-\alpha \times \frac{(\text{NDVI})_i}{\beta - (\text{NDVI})_i}\right) \quad (9)$$

式中,  $\alpha$ 、 $\beta$ 为决定NDVI- $C$ 曲线形状的参数, 大量应用表明 $\alpha = 2$ 、 $\beta = 1$ 较为理想(Van等, 2000)。总体来说, 区域尺度上利用遥感植被指数提取 $C$ 值是一种最简便和最实用的方法。

为计算海河流域2000年—2008年的平均 $C$ 因子值, 首先计算相应时间范围内的汛期(6月—10月)NDVI的平均值, 然后利用式(9)计算得到 $C$ 因子的分布图(图2(d))。

### 3.3.5 水土保持措施因子( $P$ )

水土保持措施因子 $P$ 是采取水保措施后, 土壤流失量与顺坡种植时的土壤流失量的比值(刘宝元等, 2001)。目前, 径流小区土壤侵蚀的 $P$ 因子值一般通过试验观测确定, 而在区域尺度的土壤侵蚀研究中, 则难以通过实测方法或遥感估算的方法确定相关参数值。由于土地利用/土地覆被能够一定程度反映水土保持措施差异, 因而常常采用依据土地利用类型赋值的方法确定 $P$ 值。本研究参考蔡崇法等人(蔡崇法等, 2000)的研究结果, 并结合当地土地利用及农事活动情况, 分别确定不同土地利用类型的 $P$ 值(表1)。海河流域的水土保持措施因子如图2(e)。

表1 不同土地利用类型 $P$ 值

土地利用类型	水田	旱地	林地	疏林地	其他林地	灌草地	水域	城镇居民点	裸岩
$P$ 值	0.01	0.4	1	1	0.7	1	0	0	0

## 3.4 水土流失风险评估

以上不同水土流失控制因子计算所用数据来源不同, 因而其空间尺度存在着一定的差异。为综合各水土流失因子计算水土流失风险, 首先将上述图层转化为统一坐标系下像元大小为1 km × 1 km的栅格图, 然后相乘得到海河流域不同时期的土壤侵蚀空间分布图。尽管计算结果为土壤侵蚀模数的定量结果, 但考虑到USLE应用对象及尺度的差异, 本研究综合考虑直方图的分布(图3)及其他人的研

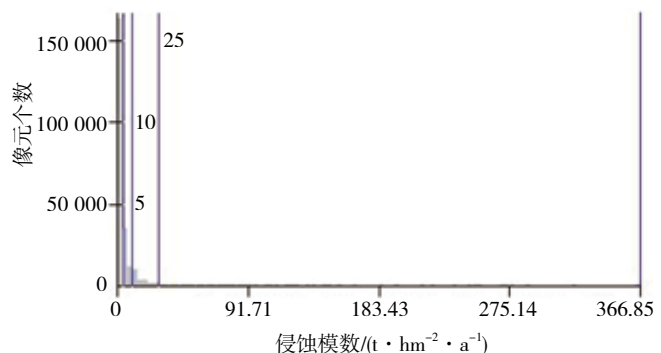


图2 海河流域土壤侵蚀模数直方图

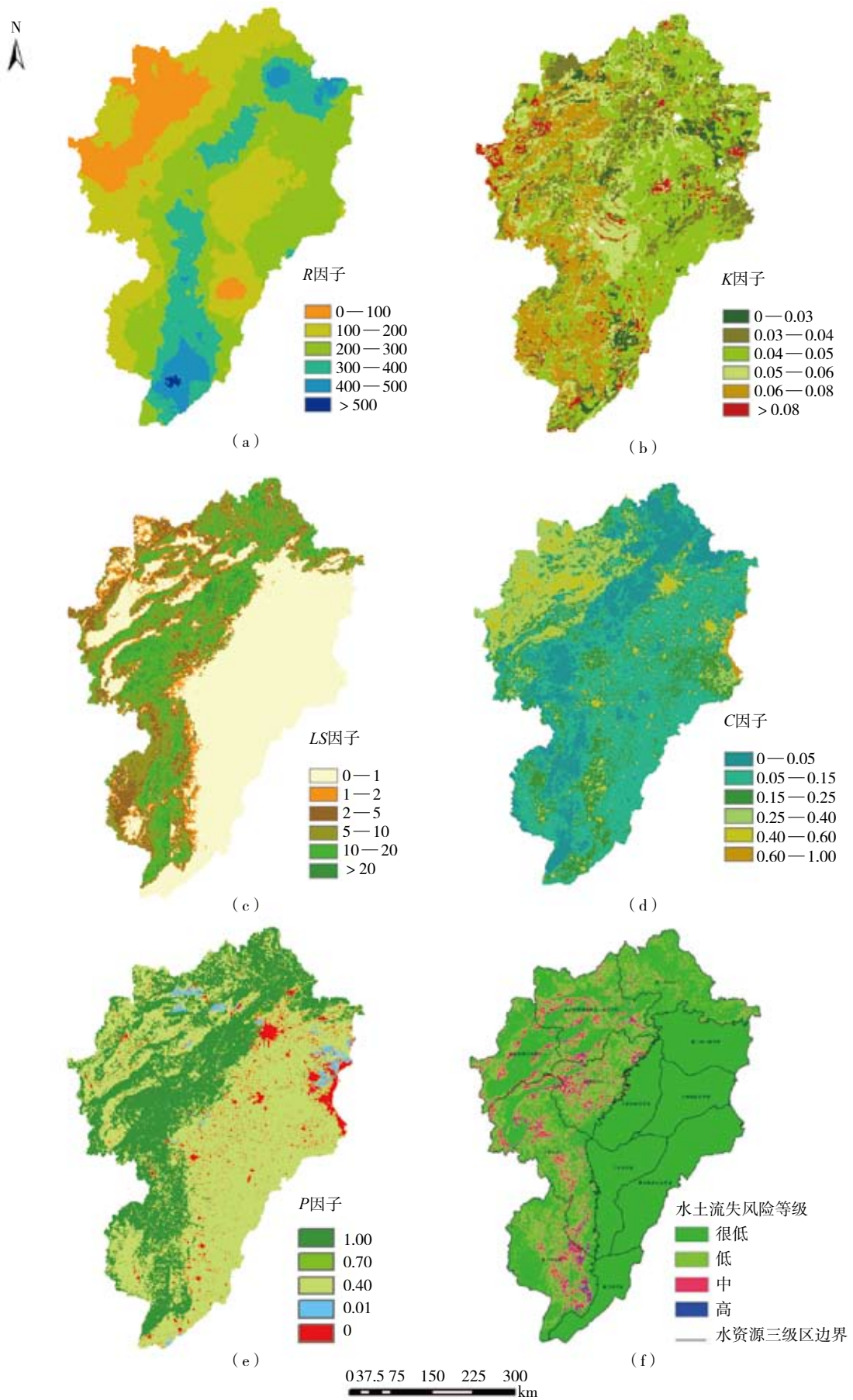


图3 侵蚀力控制因子及水土流失风险计算结果

(a) R因子; (b) K因子; (c) LS因子; (d) C因子; (e) P因子; (f) 水土流失风险等级



究成果(欧阳雪芝和潘竞虎, 2006; 李晓松等, 2010)对其进行定性化分级, 得到从低到高的水土流失风险等级, 以反映海河流域区域尺度上不同空间位置上水土流失可能发生的概率的相对高低, 并

通过对不同区域的水土流失风险等级的统计来分析区域尺度上水土流失风险的差异。海河流域水土流失风险等级的侵蚀模数阈值及不同等级面积的如表2。

表2 海河流域水土流失风险分级及统计

侵蚀模数/(t·hm <sup>-2</sup> ·a <sup>-1</sup> )	水土流失风险等级	面积/km <sup>2</sup>	比例/%
0—5	很低	159079	69.13
5—10	低	50025	21.74
10—25	中	19534	8.49
> 25	高	1480	0.64

## 4 结果与分析

### 4.1 海河流域水土流失风险空间分布

海河流域水土流失风险空间分布如图2(f)所示, 整个海河流域水土流失风险共分为“很低”、“低”、“中”、“高”4个等级。为了更好地解释海河流域水土流失风险的空间分布, 本研究将其与海河流域水资源三级区叠加进行分析。可以看出, 水土流失风险的空间分布存在一条明显的分界线, 即山区与平原之间的分界线。平原地区, 包括北三河下游平原、大清河淀东平原、大清河淀西平原、子牙河平原、黑龙港及运东平原和漳卫河平原, 水土流失风险等级均为“很低”。山区的水土流失风险则明显升高, 水土流失等级从“很低”至“很高”不等, 但以“很低”、“低”、“中”为主, 高水土流失风险有局部零星分布, 而“很高”水土流失风险则较为少见。总体来说, 北三河山区的水土流失风险等级明显要低于其他几个山区, 这一定程度表明了密云水库上

游的治理效果较好。

为了对海河流域山区水土流失风险的差异进行更好的分析, 本研究对北三河山区、永定河册田水库以上、永定河册田水库至三家店区间、大清河山区、子牙河山区和漳卫河山区等6个三级区的不同等级水土流失风险面积的分布进行了统计(表3)。可以看出, 水土流失风险高等级面积有一定分布, 最高为漳卫河山区(426 km<sup>2</sup>), 接下来依次为子牙河山区(347 km<sup>2</sup>), 大清河山区(230 km<sup>2</sup>), 永定河册田水库至三家店区间(217 km<sup>2</sup>), 而永定河册田水库以上及北三河山区级数相对较小, 分别为59 km<sup>2</sup>与28 km<sup>2</sup>, 这表明漳卫河山区、子牙河山区、大清河山区及永定河册田水库至三家店区间的水土流失风险高等级分布较多, 应该重点治理。另外, 对于不同区域中等水土流失风险以上等级比例, 大清河山区的总体水土流失风险等级最高, 比例高达21.45%, 而且低水土流失风险面积超过了很低水土流失风险面积(2519 km<sup>2</sup>);

表3 海河流域山区水土流失风险面积统计

水资源三级区(山区)	水土流失风险等级					中度以上比例/%
	很低	低	中	高	/km <sup>2</sup>	
北三河	14453	6568	932	28		4.37
大清河	6015	8534	3744	230		21.45
永定河册田水库以上	10449	4697	2102	59		12.49
永定河册田水库至三家店区间	14096	9042	3912	217		15.14
子牙河	13602	11750	4993	347		17.40
漳卫河	12725	9126	3750	426		16.05



表 4 不同坡度带水土流失风险面积统计

坡度范围	水土流失风险等级			
	很低	低	中	高
<5°	125951	9330	2192	124
5°—8°	7418	8368	2772	135
8°—15°	11749	15959	6928	405
15°—25°	9840	12056	5743	458
25°—35°	3345	3586	1538	164
>35°	433	600	297	29

子牙河山区和漳卫河山区次之，分别为17.40%与16.05%；接下来为永定河流域的册田水库至三家店区间与册田水库以上区域，分别为15.14%与12.49%，其中册田水库以上区域水土流失风险更低；北三河山区总体水土流失风险等级最低，比例仅为4.37%。总体来说，海河流域北三河山区水土流失风险最低，太行山区最高，永定河上游介于两者之间。

#### 4.2 海河流域水土流失风险空间差异分析

##### 4.2.1 水土流失风险与坡度之间的关系

坡度直接影响径流的冲刷能力，是控制水土流失发生的重要因子。为分析海河流域水资源三级区的山区不同坡度的水土流失风险情况，将坡度分为6级，分别为0°—5°，5°—8°，8°—15°，15°—25°，25°—35°，大于35°，然后与水土流失风险进行叠置分析，得到不同坡度带水土流失风险分布情况（表4）。从表4可以看出，对于不同水土流失风险等级，水土流失风险很低等级主要分布在小于5°的坡度范围，“中”、“高”水土流失风险面积主要集中在8°—15°与15°—25°两个坡度带内，其面积比例约为所有“中”、“高”级水土流失风险面积的65%；对于不同坡度带

来说，高水土流失风险等级面积所占比例随坡度的增加而增加，从0.09%增加到2.1%，这表明地形因素是导致高水土流失风险的重要因子。因此，未来海河流域水土流失治理应以坡度在8°—25°之间的治理工作为主，同时应重点关注坡度较大地区的高水土流失风险地区。

##### 4.2.2 水土流失风险与土地利用的关系

分析水土流失风险与土地利用的关系，有助于发现并识别水土流失风险较高地土地利用类型，进而可为后期的水土保持治理提供参考。将水土流失风险土层与土地利用图层进行叠置分析，获取不同土地利用类型的水土流失风险分布信息（表5）。从表5可以看出，水田的水土流失风险以“很低”为主，比例可达98.5%；“中”、“高”水土流失风险主要存在于灌草地中，约占总“中”、“高”水土流失风险面积的59.67%，值得注意的是灌草地的“低”水土流失风险面积比“很低”还要多，这表明灌草地整个土地类型易发生水土流失；其次为林地，比例约占17.96%，接下来分别为旱地和疏林地，比例分别占10.6%和9.6%。由此可知，灌草地水土流失风险等级最高，在未来的防治时应进行针对性治理。

表5 不同土地利用水土流失风险面积统计

土地利用类型	水土流失风险等级			
	很低	低	中	高
水田	526	7	1	0
旱地	87687	6746	2109	110
林地	11558	9550	3503	255
疏林地	4973	4684	1859	150
灌草地	25886	27488	11561	842
其他	28329	1518	491	46

## 5 结论与讨论

本研究借鉴USLE的因子选择及综合方法,在遥感和GIS的支撑下对海河流域的水土流失风险进行评价,得出如下结论:

(1) 海河流域水土流失风险的空间分布存在一条明显的分界线,即山区与平原之间的分界线。平原地区水土流失风险等级均为“很低”,山区的水土流失风险则明显升高,但以“很低”、“低”、“中”为主,“高”水土流失风险呈局部分布。

(2) 对于“中等”水土流失风险以上等级比例,大清河山区的总体水土流失风险等级最高,比例高达21.45%;子牙河山区和漳卫河山区次之,分别为17.40%和16.05%;接下来为永定河流域的册田水库至三家店区间与册田水库以上区域,分别为15.14%与12.49%,其中册田水库以上区域水土流失风险更低;北三河山区总体水土流失风险等级最低,比例仅为4.37%。总体来说,海河流域北三河山区水土流失风险最低,太行山区最高,永定河上游介于两者之间。

(3) 水土流失风险“很低”等级主要分布在小于 $5^{\circ}$ 的坡度的平坦地区,“中”、“高”水土流失风险面积主要集中在 $8^{\circ}$ — $15^{\circ}$ 与 $15^{\circ}$ — $25^{\circ}$ 两个坡度带内,其面积比例约为所有“中”、“高”级水土流失风险面积的65%,且“高”水土流失风险等级面积所占比例随坡度的增加而增加。

(4) 水田的水土流失风险以很低为主,比例可达98.5%;“中”、“高”水土流失风险主要存在于灌草地类型上,约占总“中”、“高”水土流失风险面积的59.67%,其次为林地,比例约占17.96%,接下来分别为旱地和疏林地,比例分别占10.6%和9.6%。由此可知,灌草地水土流失风险等级最高,在未来的防治时应进行针对性治理。

北三河山区、永定河上游及太行山区均为国家水土保持重点防治区范围,其中永定河上游治理开始时间最早(1982年),密云水库上游(北三河山区)从1989年开始治理,而太行山区则从1996年才开始全面治理(孟宪智和李子轩,2005)。水土流失的治理工作并不是一蹴而就的,而是一个渐进化的过程。受国家投入及地方经济的影响,不同区域的治理时间和治理力度均存在着一定的差异,这也决定了水土流失治理成效的差异,而这个差异则间接地反映到了本研究

水土流失风险等级的高低上面。如3.1节所述,太行山区的总体水土流失风险等级最高,这与太行山区治理起步较晚,山区面积较大,当地经济条件落后不无关系。密云水库上游所在的北三河山区尽管治理时间不如永定河上游早,但因密云水库是北京的地表饮用水源,无论国家还是北京市的投入都非常大,这可能也是现在北三河山区的总体水土流失风险低于永定河上游的原因所在。

未来海河流域山区水土流失的治理力度应继续加大,但前提是要做到科学治理,以达到事半功倍的效果。在有限资源与投入的前提下,了解哪些区域水土流失可能性相对较大、什么土地利用类型水土流失风险最高、什么地形最容易导致严重的水土流失,进而开展相应地治理与保护是进行科学水土流失防治的基础。本研究得到的海河流域水土流失风险空间分布图可以较好地回答这一系列问题,可为流域管理机构提供了决策参考。

## REFERENCES

- Cai C F, Ding S W, Shi Z H, Huang L and Zhang G Y. 2000. Study of Applying USLE and Geographical Information System IDRISI to Predict Soil Erosion in Small Basin. *Journal of soil and water conservation*, **14**(2): 19–24
- De Jong, S M, Brouwer, L C and Riezebos, H. 1998. Erosion hazard assessment in the Peyne catchment, France. Working paper DeMon-2 Project. The Netherlands: Utrecht University: 8–18
- Jorgens C and Fander M. 1993. Soil erosion assessment and simulation by means of SGEOS and ancillary digital data. *International Journal of Remote Sensing*, **14** (15): 2847–2855
- Li X S, Ji C C, Wu B F, Zeng Y and Yan N N. 2010. Dynamics of water and soil loss based on remote sensing and GIS: A case study in Chicheng County of Hebei Province. *Chinese Journal of Ecology*, **28**(9): 1723–1729
- Liu B Y, Nearing M A and Risse L M. 1994. Slope gradient effects on soil loss for steep slopes. *Transactions of the ASAE*, **37**(6): 1835–1840
- Liu B Y, Xie Y and Zhang K L. 2001. Soil Erosion Prediction Model. Beijing: China Science and Technology Press: 163–200
- Ma J W, Xue Y, Ma C F, and Wang Z G. 2003. A data fusion approach for soil erosion monitoring in the Upper Yangtze River Basin of China based on Universal Soil Loss Equation (USLE) model. *International Journal of Remote Sensing*, **24** (23): 4777–4789
- Ma Z Z. 2002. Water and soil conservation ecological construction measures layout in view of the present situation of water and soil loss in the Haihe River Basin. *Haihe water resources*, (5): 5–9
- McCool, D K, Brown L C, Foster G R, Mutchler C K and Meyer L

- D.1989.Revised slope length factor for the Universal Soil Loss Equation. *Transactions of the ASAE*, **32**(5): 1571-1576
- Meng X Z and Li Z X. 2005. Review and prospect of water and soil conservation monitoring in the Haihe Basin. *Haihe water resources*, (5): 18-20
- Ouyang X Z and Pan J H. 2006. Quantitative Study of Soil Erosion on the Longdong Loess Plateau Using GIS and RS—A Case Study of the Qingcheng Project Area. *Bulletin of soil and water conservation*, **26**(5): 75-81
- Renard K G., Foster G R, Weessies G A, McCool D K and Yoder D C. 1997. Predicting Soil Erosion by Water: A guide to conservation planning with the Revised Universal Soil Loss Equation (RUSLE). U.S. Department of Agriculture, Agriculture Handbook: 703
- United States Department of Agriculture.1990. EPIC-Erosion / productivity Impact Calculator 1. Model Documentation. Technical Bulletin Number 1768. Washington DC
- Van der Knijff J M, Jones R J A and Montanarella L. 2000. Soil Erosion Risk Assessment in Europe, EUR 19044 EN. Hannover: European Soil Bureau: 34
- Vrieling A, De Jong S M, Sterk G and Rodrigues S C. 2008. Timing of erosion and satellite data: A multi-resolution approach to soil erosion risk mapping. *International Journal of Applied Earth Observation and Geoinformation*, **10**(3): 267-281
- Wang W Z. 1995. Study on rainfall erosivity in China. *Journal of soil and water conservation*, **9**(4): 5-18
- Wischmeier W H and Smith D D. 1978. Predicting rainfall erosion losses—a guide for conservation planning. U.S. Department of Agriculture, Agriculture Handbook: 537
- Zhang K L, Peng W Y and Yang H L. 2007. Soil erodibility and its estimation for agricultural soil in China. *Acta Pedologica Sinica*, **44**(1): 7-13

### 附中文参考文献

- 蔡崇法, 丁树文, 史志华, 黄丽, 张光远. 2000. 应用USLE模型与地理信息系统IDRISI预测小流域土壤侵蚀量的研究. 水土保持学报, **14**(2): 19-24
- 李晓松, 姬翠翠, 吴炳方, 曾源, 闫娜娜. 2010. 基于遥感和GIS的水土流失动态监测研究—以河北省赤城县为例. 生态学杂志, **28**(9): 1723-1729
- 刘宝元, 谢云, 张科利. 2001. 土壤侵蚀预报模型. 北京: 中国科学技术出版社: 163-200
- 马志尊. 2002. 从海河流域水土流失现状谈水土保持生态建设措施布局. 海河水利, (5): 5-9
- 孟宪智, 李子轩. 2005. 海河流域水土保持监测工作与展望. 海河水利, (5): 18-20
- 欧阳雪芝, 潘竞虎. 2006. 陇东黄土高原土壤侵蚀变化定量遥感监测—以黄土高原水保二期世行贷款庆城项目区为例. 水土保持通报, **26**(5): 75-81
- 王万忠. 1995. 中国降雨侵蚀力R值的计算与分布. 水土保持学报, **9**(4): 5-18
- 张科利, 彭文英, 杨红丽. 2007. 中国土壤可蚀性值及其估算. 土壤学报, **44**(1): 7-13